CSEE Journal of Power and Energy Systems, Available online August 2019
DOI: 10.17775/CSEEJPES.2019.00320
This article has been accepted for publication in a future issue of this journal, but has not been fully edited. Content may change prior to final publication.

Chance-constrained Optimal Dispatch of Integrated Electricity and Natural Gas Systems Considering Medium and Long-term Electricity Transactions

Gang Wu, Yue Xiang, *Member*, *IEEE*, Junyong Liu, *Member*, *IEEE*, Xin Zhang, *Member*, *IEEE*, and Shuoya Tang

***Abstract*—A novel stochastic optimal dispatch model, considering medium and long-term electricity transactions for a wind power integrated energy system using chance constrained programming, is proposed. The electricity contract decomposition problem is introduced into the day-ahead optimal dispatch plan formulation progress. Considering the case that decomposition results may be not executable in the dispatch plan, a coordinated optimization strategy based on the Lagrange multiplier is proposed eliminate the non-executable electric quantity. At the same time, the uncertainties and correlation of wind power are considered in the dispatch model, and the original stochastic dispatch problem is transformed into a mixed integer second-order cone programming problem using second-order cone relaxation and sample average approximation approach. Case study results demonstrate the validity of the proposed method.**

***Index Terms*—Electricity transaction, wind power, uncertainties, chance-constrained programming.**

I. Introduction

At present, the day-ahead and spot market trading platforms have not been established in China, and the electricity trading is dominated by the medium and long-term electricity market [1]. During the current transition period, market participants, such as generation suppliers, can sign medium or long-term contract and dispatch center is primarily responsible for the decomposition of contracted energy [2]. In this situation, dispatch center needs to determine a coordinated optimization strategy between contract energy decomposition and generation dispatch plan formulation. However, there is usually a serious contradiction between daily dispatch plan formulation and contract completion progress schedule requirements. How to mitigate this conflict and realize coordinated optimization between contract decomposition and dispatch plan formulation is still a tough problem that needs to be solved.

This work was supported in part by the National Natural Science Foundation of China (51807127), in part by the Fundamental Research Funds for Central Universities (YJ201654). (*Corresponding author: Yue Xiang.*)
G. Wu, Y. Xiang, J. Liu, S. Tang are with Sichuan University, Chengdu, 610065, China(email: scu_gw@163.com, xiang@scu.du.cn, liujy@scu.du.cn, tangsy@stu.scu.edu.cn)
X. Zhang is with Energy and Power Theme, School of Water, Energy and Environment, Cranfield University, Cranfield, MK43 0AL, UK (email: xin.zhang@cranfield.ac.uk)
DOI: 10.17775/CSEEJPES.2019.00320

During the electricity market transition period, many studies have been done on the optimal generation dispatch considering electricity transaction plans. In [3], a month security constrained unit commitment (SCUC) model considering the contracted energy completion deviation of different units was proposed, which achieved optimal coordination of electricity contract delivery and month dispatch plan formulation. Nevertheless, due to the influence of renewable energy and load demand uncertainties, the transaction completion schedule obtained from the SCUC month model are often non-executable in the actual daily dispatch plan. As a result, the delivery of the electricity contract into the daily dispatch plan will become a continual issue within the electricity market operation. In order to cope with this challenge, a security constrained unit commitment week model for coordinating between electricity transaction plans and dispatch plans formulation was presented in [1], which avoids this conflict to some extent. Furthermore, the contract decomposition problem was considered in the procedures of a day-ahead dispatch plan formulation in [2], which achieved the nested optimization of the electricity transaction plan and dispatch plan formulation. However, the case that the daily decomposed electric quantity of contract may not be executable is ignored.

In the meantime, due to the rapid growth of gas-fired units and renewable generation [4]-[5], the security of the power system is challenged by gas network constraints and renewables uncertainties [6]-[8]. These factors should be reasonably considered in dispatch plan formulation. The scenario-based stochastic optimization and robust optimization dispatch models for integrated energy systems (IESs) were constructed in [5],[6],[8] respectively, where the impact of wind power uncertainties on the energy flow and operational costs were analyzed. However, the scenario-based stochastic optimization relies on a certain number of scenarios to represent the stochastic characteristic of uncertain factors, which may cause inaccurate results [9]. Robust optimization is an effective way to achieve optimal dispatch the under worst-case scenario of multiple uncertain variables, but its decision results are usually conservative, which would inevitably result in high operational costs and low utilization rates of renewable generation [10]-[11].

Chance-constrained programming (CCP) is another way to resolve uncertainty [12]-[13], and has drawn great attention in recent years. An acceptable probability level is predefined to describe constraint violation, and the CCP optimal problem can be solved with probabilistic constraints transforming into the

equivalent deterministic forms [14]. The CCP method has been widely used in unit commitment [15], optimal power flow [16], and in energy management [17] in power systems. However, it has not been applied to integrated electricity and natural gas systems (IEGSs) considering the correlation of multiple uncertain factors.

To overcome the above issues, a novel stochastic optimal dispatch model of IEGSs based on chance-constrained programming is proposed in this paper. The electricity contract decomposition problem is involved in the optimal dispatch plan formulation procedure. Considering the case that decomposition results may be not executable, a coordinated optimization strategy is presented in this paper to provide relatively practical contract decomposition results, so as to improve the feasibility of the delivery of electricity transaction plan into the actual dispatch plan. Moreover, uncertainties and correlation of multiple wind farm's power output are involved in this paper. The probabilistic chance constraints are transformed into deterministic forms based on a sample average approximation approach. The IEGS operation can realize a balanced tradeoff between system operational costs, wind power utilization rates and reliability through properly choosing the confidence levels.

The rest of this paper is organized as follows. An optimal dispatch model of IEGSs is presented in Section II, followed by the equivalent deterministic transformation of probabilistic constraints in Section III and a solution procedure in Section IV. In Section V, simulation results are displayed to demonstrate the validity of the proposed method. Conclusions are given in Section VI.

II. Optimization Model

A. Objective Function

The gas-fired units would perform as key coupling devices that interface the electricity and natural gas systems. The objective function (1) is to minimize the total operational costs including (*i*) generation costs of the conventional units, (*ii*) the natural gas contract costs for gas-fired units, (*iii*) generator's start-up and shutdown costs and (*iv*) reserve capacity costs.

$$\min f = \sum_{t=1}^{T}\Big(\sum_{i=1}^{N_E}\underbrace{F_{i,e}(P_{i,t})I_{i,t}}_{i}+\sum_{i=1}^{N_G}\underbrace{C_{i,g}F_{i,g}(P_{i,t})I_{i,t}}_{ii}+\sum_{i=1}^{N_E\cup N_G}\underbrace{(SU_{i,t}+SD_{i,t})}_{iii}+\underbrace{F_{i,t}^{\mathrm{res}}}_{iv}\Big) \tag{1}$$

in which

$$F_{i,g}(P_{i,t})=\alpha_{i,g}+\beta_{i,g}P_{i,t}+\gamma_{i,g}(P_{i,t})^2,\quad \forall t \tag{2}$$

$$F_{i,e}(P_{i,t})=\alpha_{i,e}+\beta_{i,e}P_{i,t}+\gamma_{i,e}(P_{i,t})^2,\quad \forall t \tag{3}$$

$$F_{i,t}^{\mathrm{res}}=C_i^{\mathrm{u}}R_{i,t}^{\mathrm{u,r}}+C_i^{\mathrm{d}}R_{i,t}^{\mathrm{d,r}},\quad \forall t \tag{4}$$

where N_E and N_G are the number of conventional units and gas-fired units respectively. $I_{i,t}$ is the indicator of the unit's work status. $\alpha_{i,g}$, $\beta_{i,g}$ and $\gamma_{i,g}$ indicate the gas consumption coefficients of the unit *i*. $\alpha_{i,e}$, $\beta_{i,e}$ and $\gamma_{i,e}$ are the generation cost coefficients of the conventional unit *i*. $C_{i,g}$, C_i^{u} and C_i^{d} denote the gas purchase price, and upward and downward reserve capacity price. $R_{i,t}^{\mathrm{u,r}}$ and $R_{i,t}^{\mathrm{d,r}}$ represent the upward and downward reserve capacity offered by the generator (*i*).

B. Power System Constraints

1) Unit Capacity Limits

$$I_{i,t}P_i^{\min}\le P_{i,t}\le I_{i,t}P_i^{\max},\ \forall\, i,\forall t \tag{4}$$

where $P_i^{\max}$ and $P_i^{\min}$ indicate the upper and lower power output limits of the generator (*i*).

2) Ramp Rate Limits

$$P_{i,t}-r_i^{\mathrm{d}}\le P_{i,t+1}\le P_{i,t}+r_i^{\mathrm{u}},\ \ \forall\, i,\forall t \tag{5}$$

where r_i^{d} and r_i^{u} denote the ramping rate of the generator (*i*).

3) Minimum On/Off Time Limits

$$\begin{aligned}&(X_{i,t-1}^{\mathrm{on}}-T_i^{\mathrm{on}})(I_{i,t-1}-I_{i,t})\ge 0,\ \ \forall\, i,\forall t\\&(X_{i,t-1}^{\mathrm{off}}-T_i^{\mathrm{off}})(I_{i,t}-I_{i,t-1})\ge 0,\ \ \forall\, i,\forall t\end{aligned} \tag{6}$$

where $X_{i,t}^{\mathrm{on}}$ *and* $X_{i,t}^{\mathrm{off}}$ represent the continuous ON/OFF time of the generator (*i*) at time *t*, respectively. T_i^{on} *and* T_i^{off} indicate the minimum allowable continuous operation and shutdown time.

4) Daily Execution Electric Quantity Limits

For the units that have signed electricity contracts, the daily execution power quantity limits should be considered, which are shown as follows:

$$\sum_{t=1}^{T}P_{i,t}\Delta_t=E_i^x,\ \ i\in N_{\mathrm{b}} \tag{7}$$

where E_i^x represents the daily plan power quantities of unit *i* that should be completed (obtained from electricity contract decomposition results). N_{b} is the set of units that have signed electricity contracts.

C. Chance-Constraints of Power Systems

The chance-constrained programming is utilized to model the influence of uncertain factors on the load balance, reserve and power flow constraints.

1) Load Balance Constraints

$$\sum_{i=1}^{N_E}P_{i,t}+\sum_{i=1}^{N_G}P_{i,t}+\Omega\Big(\sum_{w=1}^{W}P_{w,t}\Big)=\sum_{d=1}^{N_D}DL_{d,t} \tag{8}$$

where $P_{i,t}$ and $P_{w,t}$ indicate the power output of the units (including gas-fired and conventional units) and wind farms. $DL_{d,t}$ represents the demand of load *d*. *W* and N_{D} denote the number of wind farms and load. $\Omega(\cdot)$ represents the total wind power output functions. Due to the wind power uncertainties, constraint (8) can be converted to probabilistic forms as follows:

$$P_{rob}\Big\{\sum_{i=1}^{N_E}P_{i,t}+\sum_{i=1}^{N_G}P_{i,t}+\sum_{w=1}^{W}P_{w,t}\ge\sum_{d=1}^{N_D}DL_{d,t}\Big\}\ge\beta_1,\ \ \forall t \tag{9}$$

where β_1 denotes the confidence level that represents total unit output meeting total load demand.

2) Reserve Constraints

The spinning reserve constraints (10)-(11) are modeled in this paper to control the risk caused by wind power uncertainties.

$$P_{rob}\Big\{\sum_{i=1}^{N_E\cup N_G}R_{i,t}^{\mathrm{u,r}}\ge R_t^{\mathrm{u}}+\alpha^{\mathrm{u}}\sum_{w=1}^{W}P_{w,t}\Big\}\ge\beta_2,\ \ \forall t \tag{10}$$

$$P_{rob}\{\sum_{i=1}^{N_E\cup N_G} R_{i,t}^{d,r} \geq R_t^d + \alpha^d \sum_{w=1}^{W}(P_w^{rate} - P_{w,t})\} \geq \beta_3,\ \forall t \quad (11)$$

where P_w^{rate} denotes the maximum or rated power output of wind farm w. R_t^u and R_t^d are the system upward and downward reserve capacity demand at time t, 5% of load demand at current period t is adopted in this paper. α^u and α^d are the up and down reserve demand coefficients for wind power, 10% is adopted in this paper. β_2 , β_3 represent the confidence level that the total provided reserve capacity meets the reserve demand.

3) Power Transmission Flow Constraints

$$P_{rob}\{\sum_{i=1}^{N_E} GSF_{l,i}P_{i,t} + \sum_{i=1}^{N_G} GSF_{l,i}P_{i,t} + \sum_{w=1}^{W} GSF_{l,w}P_{w,t} - \sum_{d=1}^{D} GSF_{l,d}DL_{d,t} \leq P_l^{max}\} \geq \beta_4, \forall l, \forall t \quad (12)$$

$$P_{rob}\{\sum_{i=1}^{N_E} GSF_{l,i}P_{i,t} + \sum_{i=1}^{N_G} GSF_{l,i}P_{i,t} + \sum_{w=1}^{W} GSF_{l,w}P_{w,t} - \sum_{d=1}^{D} GSF_{l,d}DL_{d,t} \geq -P_l^{max}\} \geq \beta_5, \forall l, \forall t \quad (13)$$

where $GSF_{l,i}$, $GSF_{l,w}$ and $GSF_{l,d}$ denote the generation shift factor of the generation unit, wind farm and load demand based on the DC power flow model. P_l^{max} denotes the maximum transmission power of line l. β_4 , β_5 represent the confidence level that meets the power flow security demand.

D. Natural Gas System Constraints

1) Node Gas Pressure Constraint

$$\pi_i^{min} \leq \pi_{i,t} \leq \pi_i^{max},\ \forall t,\ \forall i \in N_{gas} \quad (14)$$

where π_i^{max} and π_i^{min} denote upper and lower limits of the gas pressure. N_{gas} is the set of the natural gas node.

2) Gas Flow Constraints

$$F_{ij}^2 = \mathrm{sgn}(\pi_i, \pi_j)C_{ij}^2(\pi_i^2 - \pi_j^2),\ \forall (i,j) \in N_{gas} \quad (15)$$

$$\mathrm{sgn}(\pi_i, \pi_j) = \begin{cases} +1 & \pi_i \geq \pi_j \\ -1 & \pi_i < \pi_j \end{cases} \quad (16)$$

where F_{ij} represents the gas flow through pipeline ij. C_{ij} is the comprehensive parameters of the pipeline characteristics.

3) Gas Supplier Constraint

$$F_{j,min}^{sp} \leq F_{j,t}^{sp} \leq F_{j,max}^{sp} \quad (17)$$

where $F_{j,min}^{sp}$ and $F_{j,max}^{sp}$ are lower and upper gas output bounds of supplier j.

4) Nodal Load Balance Constraint

$$F_{j,t}^{sp} - F_{j,t}^{gas} - F_{j,t}^{L} + \sum_{i\in j} F_{ij,t} = 0,\ \forall t \quad (18)$$

where $F_{j,t}^{L}$ *and* $F_{j,t}^{gas}$ are the gas demand of conventional gas load and gas-fired generators at node j.

E. Constraints of Coupling Devices and System Emission

1) Constraints of Gas-Fired Units

The gas demand of the gas-fired unit is considered as a load for natural gas system, which must be less than or equal to the natural gas day contract limit (19)

$$\sum_{t=1}^{T} F_i^g(P_{i,t}) \leq F_i^{max} \quad (19)$$

where F_i^{max} is the contracted maximum natural gas consumption for gas-fired generator (i).

2) Emission Constraints

The total pollution gas emission of all units during the scheduling horizon must not exceed the maximum emission levels, which are represented by

$$\sum_{t=1}^{T}\sum_{j\in J}\sum_{i=1}^{N_E}(F_{i,j,t}^e(P_{i,t})\cdot I_{i,t} + SU_{i,j,t}^e + SD_{i,j,t}^e) + \sum_{t=1}^{T}\sum_{i=1}^{N_G}(F_{i,t}^g(P_{i,t})\cdot I_{i,t} + SU_{i,t}^g + SD_{i,t}^g) \leq \mathrm{ES}^{max} \quad (20)$$

in which

$$F_i^g(P_{i,t}) = a_i^g + b_i^g P_{i,t} + c_i^g (P_{i,t})^2 \quad (21)$$

$$F_{i,j}^e(P_{i,t}) = a_{i,j}^e + b_{i,j}^e P_{i,t} + c_{i,j}^e (P_{i,t})^2 \quad (22)$$

where a_i^g ,$b_{i,}^g$and c_i^g represent the gas-fired generator (i) carbon emission coefficients. $a_{i,j}^e$, $b_{i,j,}^e$ $c_{i,j}^e$ represent the pollution gas emission coefficients of conventional unit. J is the set of pollution gas type (including SO_2,NO, CO_2). SU_i^g and SD_i^g represent the gas-fired generator (i) start-up and shutdown carbon emissions, respectively. $SU_{i,j}^e$ and $SD_{i,j}^e$ represent the start-up and shutdown pollution gas emission of conventional unit i, respectively. ES^{max} is the maximum pollution gas emission levels.

III. Deterministic Transformation of Chance Constraints Considering Correlation of Wind Power

Constraints (9)-(13) are probability forms when the chance-constrained programming is utilized, which introduces the difficulties in solving the optimal dispatch model. Generally, these probability constraints can be converted to deterministic expressions based on the cumulative distribution function (CDF). However, for multiple wind farms considering wind power correlation, the joint cumulative distribution function is difficult or even impossible to obtain. The copula function is an effective way to describe correlation characteristics between uncertain factors, which has been widely used in power systems [18,19]. Nevertheless, the procedure of obtaining the copula function expression is relatively complex. Thus, a deterministic transformation method of chance constraints based on sample average approximation approach considering wind power correlation is proposed. It should be noted that the correlation of wind power is not directly modeled in this paper, but rather we use modeling of the correlation of wind speed combined with the relationship between wind speed and wind power to reflect the wind power correlation.

A. Sample Matrix Considering the Correlation of Wind Speed

The actual wind speed can be seen as the sum of the forecasting values and forecasting errors, which can be represented by (23):

$$v_w(t) = V_w(t) + \varepsilon_w(t) \quad (23)$$

where $V_w(t)$ denotes the forecasting values. $\varepsilon_w(t)$ represents the forecasting errors. The wind speed forecasting error is usually subject to a normal distribution in the daily scheduling horizon. A widely used standard normal distribution is adopted in this

paper.

The wind speed between wind farms of close geographical location demonstrates a strong correlation characteristic, and the correlation usually varies with time. Therefore, the time-varying correlation coefficient matrix can be used to describe this correlation characteristic [6].

In the actual day-ahead scheduling model, a set of determined wind speed sequences can be determined by the wind speed forecast method. However, there would be errors in the wind speed forecasting, so the randomness and correlation of wind speed forecasting errors are considered in this paper. The detailed method is shown as follows.

1) Time-Varying Correlation Coefficient Matrix

Historical wind speed data is used to calculate the correlation coefficients between different wind farms based on the Pearson linear correlation method [6,20]. Auto-correlation coefficients are equal to 1.

$$C_{XY}(t)=\frac{E[(X(t)-\mu(X(t)))(Y(t)-\mu(Y(t)))]}{\sigma_{X(t)}\sigma_{Y(t)}} \quad (24)$$

The correlation matrix during a certain period can be obtained according to the $C_{XY}(t)$. Taking three wind farms as an example, correlation coefficient matrix can be represented by

$$\Omega=\begin{bmatrix} 1 & C_{XY} & C_{XZ} \\ C_{YX} & 1 & C_{YZ} \\ C_{ZX} & C_{ZY} & 1 \end{bmatrix} \quad (25)$$

According to the correlation matrix, Cholesky decomposition can be used to generate correlated sample series, represented by (26)

$$\Omega=LL^{*} \quad (26)$$

2) Latin Hypercube Sampling

After the above steps, a sample matrix satisfying the desired correlation level can be obtained by utilizing the Latin hypercube sampling (LHS) and lower triangular matrix L. Detailed procedures to implement LHS can be found in [20].

B. Deterministic Transformation of Chance Constraints Based on Sample Matrix

By superimposing the forecasting error sample matrix obtained from LHS with the wind speed forecasting value, a wind speed random sample matrix $\boldsymbol{V}_w$ is determined. The number of rows of $\boldsymbol{V}_w$ represents the number of wind farms, and the number of columns denotes the number of wind speed sample data. Combined with the relationship between wind power output and wind speed [9], the sample matrix $\boldsymbol{W}_w$ of wind farm output power $P_{w,t}$ can be obtained, where the row i-th vector of the matrix is the i-th wind farm power output sample. Then the sample vectors $\boldsymbol{W}_{\mathrm{GW}}$ and $\boldsymbol{W}_{\mathrm{LW}}$ of the random variables $\sum_{w=1}^{W}P_{w,t}$ and $\sum_{w=1}^{W}GSF_{l,w}P_{w,t}$ can be calculated based on $\boldsymbol{W}_w$, which are shown as equations (27) and (28):

$$\boldsymbol{W}_{\mathrm{GW}}=\sum_{w=1}^{W}\boldsymbol{W}_w \quad (27)$$

$$\boldsymbol{W}_{\mathrm{LW}}=\sum_{w=1}^{W}\mathrm{GSF}_{l,w}\boldsymbol{W}_w \quad (28)$$

The sample matrix $\boldsymbol{W}_{\mathrm{GW}}$ is $1\times N_{\mathrm{sample}}$ dimensional matrix, $\boldsymbol{W}_{\mathrm{LW}}$ is $N_{\mathrm{e\_line}}\times N_{\mathrm{sample}}$ dimensional matrix. Where N_{sample} denotes the number of samples, $N_{\mathrm{e\_line}}$ denotes the number of transmission lines in the electricity network.

According to the sample matrix, the probabilistic constraints can be converted to deterministic forms. Taking upward spinning reserve constraints as an example, the reserve constraints can be transformed into (29)-(30):

$$W_{\mathrm{r,up}}^{s}=\begin{cases} 1, & \sum_{i=1}^{N_{\mathrm{E}}\cup N_{\mathrm{G}}}R_{i,t}^{\mathrm{up,r}}\geq R_t^{\mathrm{u}}+\alpha^{\mathrm{u}}W_{GW}^{s} \\ & \forall t,s=1,2,\cdots,N_{\mathrm{sample}} \\ 0, & \text{others} \end{cases} \quad (29)$$

$$\sum_{s=1}^{N_{\mathrm{sample}}}W_{\mathrm{r,up}}^{s}\geq\beta_2 \quad (30)$$

where W_{GW}^{s} is the s^{th} sample value of matrix $\boldsymbol{W}_{\mathrm{GW}}$. $W_{r,up}^{s}$ is 0-1 variable. With this transformation, the chance constraint (10) is substituted by $2N_{\mathrm{sample}}$ mixed integer linear constraints. However, when sample number N_{sample} is larger, the computation time will sharply increase. Thus, an equivalent substitution method based on the rank method in [12] is adopted here to achieve fast transformation. Based on the rank method in [12], the (29)-(30) could be simplified as (31)-(32).

$$\sum_{i=1}^{N_{\mathrm{E}}\cup N_{\mathrm{G}}}R_{i,t}^{\mathrm{up,r}}\geq R_t^{\mathrm{u}}+\alpha^{\mathrm{u}}\boldsymbol{W}_{\mathrm{sort,GW}}(\mathrm{ceil}(N_{\mathrm{sample}}\beta_2)),\quad\forall t \quad (31)$$

$$\boldsymbol{W}_{\mathrm{sort,GW}}=\mathrm{sort}(\boldsymbol{W}_{\mathrm{GW}})=\mathrm{sort}([W_{\mathrm{GW},t}^{1},W_{\mathrm{GW},t}^{2},\cdots,W_{\mathrm{GW},t}^{s},\cdots W_{\mathrm{GW},t}^{N_{\mathrm{sample}}}]) \quad (32)$$

where ceil () is the round up function, and sort () is the ascending sort function.

Other probability constraints can be similarly transformed into deterministic forms.

IV. Solution Procedure

The quartic functions and minimum ON/OFF time limits are linearized by the method in [21] and [22], respectively. The convex relaxation method for gas flow constraints (15)-(16) is shown in the Appendix.

In the solution process, the electricity contract decomposition model is first introduced. The obtained daily plan electric quantity is regarded as constraints of the bidding units (shown in (7)) to ensure the effective delivery of the contract. When the decomposed electric quantity is not executable in the dispatch plan, a coordinated optimization strategy between electricity contract decomposition and dispatch plan formulation is designed to deal with this challenge.

A. Electricity Contract Decomposition Model

The electricity contract decomposition model must consider factors such as contract completion progress, load profile and so on to ensure the consistent delivery of contracts. A widely used contract decomposition model for minimizing contracts completion progress differences [2] is adopted in this paper.

$$\min S(l)=\frac{1}{n_{\mathrm{b}}}\sum_{i\in N_b}(l_{i,x}-\overline{l}_x)^2 \quad (33)$$

$$\text{s.t.}\quad E_{i,x}^{\min} \le E_{i,x} \le E_{i,x}^{\max},\quad \forall i \in N_b \tag{34}$$

$$E_{i,x} + E_{i,x-1}^{o} \le E_i^{\text{trade}},\quad \forall i \in N_b \tag{35}$$

$$\sum_{i \in N_b} E_{i,x} = E_x^{\text{plan}} \tag{36}$$

$$\left| l_{i_1,x} - l_{i_2,x} \right| \le \sigma,\ i_1 \ne i_2 \tag{37}$$

in which

$$l_{i,x} = \frac{E_{i,x} + E_{i,x-1}^{o}}{E_i^{\text{trade}}} \times 100\% \tag{38}$$

$$\overline{l_x} = \frac{1}{n_{\text{b}}} \sum_{i \in N_{\text{b}}} l_{i,x} \times 100\% \tag{39}$$

$$E_x^{\text{plan}} = \frac{\sum_{i \in N_{\text{b}}} E_i^{\text{trade}} - \sum_{i \in N_{\text{b}}} E_{i,x-1}^{\text{o}}}{\sum_{i=x}^{L} D_i} \times D_x \tag{40}$$

where n_{b} is the number of units for the signed electricity contract. x denotes the plan day number. E_i^{trade} is the total contracted electric quantity of bidding unit i. $E_{i,x-1}^{o}$ represents the electric quantity that have been completed. $E_{i,x}$ denotes the daily plan electric quantity of the unit i. $E_i^{\max}$ and $E_{i,x}^{\min}$ are the maximum and minimum decomposed electric quantity, which can be obtained according to the maintenance plan, technical parameters of the unit and so on. $l_{i,x}$ denotes the unit (i) contract completion progress. $\overline{l_x}$ represents the average contract completion progress of all bidding units. E_x^{plan} denotes the electric quantity that needs to be finished on the plan day. D_x represents the load demand of the plan day. L denotes the total number of days during the contract period

Equation (33) adopts variances to represent the differences of the electricity contract completion progress between units. Equation (34) bounds the minimum and maximum execution electric quantity of unit i. Equation (35) indicates that total execution electric quantity cannot exceed the contracted energy. Equation (36) denotes the constraints of the total daily execution electric quantity of all bidding units. Equation (37) denotes that the differences of the contract completion progress of different units which must not exceed the allowable deviation margin σ .

B. Coordinated Optimization Strategy

The above established contract decomposition model is introduced to the procedure of day-ahead plan formulation in this paper. However, there are cases that the obtained decomposed electric quantity of units may not be executable in the dispatch plan. Thus, a coordinated optimization strategy is proposed to cope with this challenge.

The key idea of this coordinated optimization strategy is to introduce a slack variable to relax the daily electric quantity execution constraint (7), and the slack variable results can directly reflect the part of the daily decomposed electric quantity that cannot be executed. Then apply an iteration strategy between the contract decomposition and optimal dispatch plan formulation to eliminate the non-executable electric quantity. The detailed procedure is demonstrated as follows:

Step 1: Solve the electricity contract decomposition model and output of the daily plan electric quantity of bidding units.

Step 2: Determine the unit number for the decomposed electric quantity that is non-executable. Relax the constraints in (7) with the slack variable μ_i (41). The objective (1) is reformulated as (42)

$$\sum_{t=1}^{T} P_{i,t}\Delta_t + \mu_i = E_{i,x},\quad \mu_i \ge 0,\quad i \in N_{\text{b}} \tag{41}$$

$$\min F = f + M \sum_{i \in N_{\text{b}}} \mu_i \tag{42}$$

where f represents the original objective (1). M denotes a large positive number.

Solve the optimal dispatch model and output of the results. If μ_i is larger than zero, the daily decomposed electric quantity of unit i is not executable in the dispatch plan. The size of μ_i can reflect the part of the daily decomposed electric quantity that cannot be executed.

Step 3: Modify the decomposed electric quantity. The daily execution electric quantity constraints of the bidding units in (34) are reformulated as (43). The electricity contract decomposition model is solved again to obtain a new decomposed electric quantity of unit i.

$$E_{i,x}^{\min} \le E_{i,x} \le E_{i,x}^{1} - \mu_i,\ \ if\ \ \mu_i > 0 \tag{43}$$

$E_{i,x}^{1}$ is the decomposed electric quantity at the last time.

Step 4: Determine the feasibility of the delivery of new electricity contract decomposition results into the dispatch plan. Substituting the new decomposed energy into the constraints (7) in the optimal dispatch model, if μ_i equals zero, the procedure is terminated. If not, the above steps are repeated until the non-executable electric quantity is eliminated. In order to reduce the iteration numbers and improve solution efficiency, a threshold value $\mu_{\min}$ is set to 20. With the slack variable optimization results $\mu_i \ge \mu_{\min}$, the decomposed electric quantity is judged to be non-executable. Fig. 1 demonstrates the flowchart of the coordinated optimization strategy.

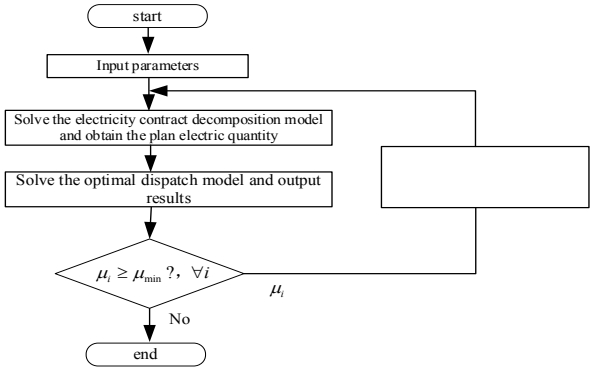

Fig. 1 Flowchart of the coordinated optimization strategy

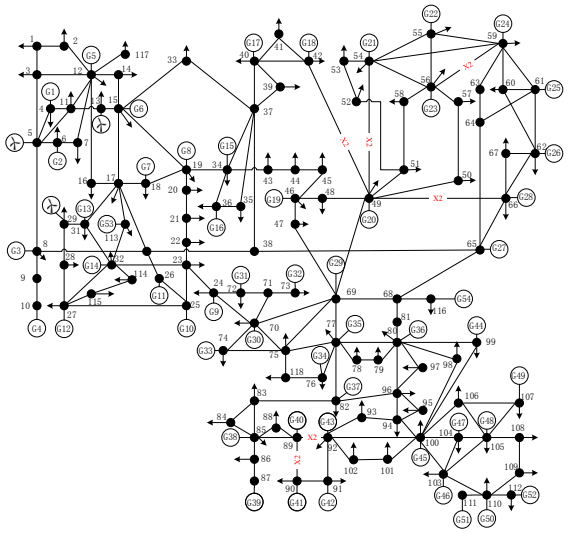

(a) IEEE 118-bus electricity network

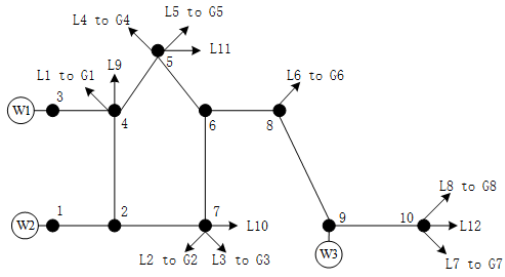

(b) 10-node natural gas network

Fig. 2 Topology of the Simulation System

V. Illustrative Example

The electricity contract decomposition model and optimal dispatch model are solved by using the CPLEX solver on a MATLAB R2014a platform. A modified IEEE 118-bus electricity network and 10-node gas network are used as the test system, which is shown in Fig. 2. The basic data of the test system can be found in [5], some price parameters, wind speed forecasting values and electricity transaction parameters can be found in [23]. The cutting in, cutting out and rated wind speed are 4, 20 and 15m/s respectively. Historical wind speed data for the same month in three different regions of the National Oceanic and Atmospheric Administration from 2003 to 2012 are utilized for analysis [24].

A. Correlation of Wind Power

1) Influence of Wind Power Correlation

In order to analyze the influence of wind power correlation on the optimal dispatch results of the IEGSs, the decomposition problem of the electricity contract is not considered in this occasion. Two types of test cases are designed as follows:

Case I: the wind power correlation is ignored.

Case II: the wind power correlation is considered.

The confidence level β_1 is set to 90%. The confidence level β_i (i=2,3,4,5) is set to 96%. The hourly correlation coefficient of different wind farms obtained from the analysis of historical data in the same month is shown in Fig. 3. Table I presents the comparison of system operational costs and total scheduled wind power in three typical wind speed environments: normal, high and low wind speed periods. It can be observed that the total operational cost in Case I is always lower than that in Case II in all wind speed environments, and the total scheduled wind power is always higher than that in Case II. In addition, from the comparison results under different confidence levels (as depicted in Fig. 4), the operational costs and scheduled wind power in Case I and Case II under different confidence levels are evidently different from each other.

The above results demonstrate that the correlation among wind farms would have certain impacts on the scheduling results, which should be taken into account in the dispatch plan formulation process to obtain a more accurate uncertainty modeling and scheduling results.

2) Influence of Different Confidence Levels

The forecasting wind speed values in the normal wind speed period are used for the analysis of the following cases. When the confidence level β_i (i=2,3,4,5) is set to 96%, and the confidence level of power balance β_1 is set to different values, the obtained total system operational cost and scheduled wind power results are depicted in Fig.4. With the confidence level β_1 increased from 60% to 95%, the total wind power output gradually decreases from 5,494 MW to 4,459 MW in Case I (W-Case I) and 5,396 MW to 3,907 MW in Case II (W-Case II), and the system operational costs increase from \$1,954,050 to \$1,986,299 in Case I (O-Case I) and \$1,957,607 to \$2,009,261 in Case II (O-Case II). The reason is that the confidence level represents the operational risk. A larger β_1 means the reduced risk brought by wind power uncertainties, which would inevitably decrease the total scheduled wind power and increase the operational costs. On the contrary, a smaller β_1 will result in lower operational costs and larger scheduled wind power, but the risk caused by wind power uncertainties is higher.

The relationship between the total system operational cost and confidence levels β_2, β_3, β_4 and β_5 is shown in Fig. 5, in which the confidence level β_1 is set to 90% and the confidence levels β_i (i=2,3,4,5) is set to the same value. The operational cost will continue to increase with the reserve and line security confidence levels varied from 90% to 98%. Although the system economy is deteriorated, the reliability of the system operation is increased.

The above analysis demonstrates that choosing the confidence level is practical significant for the IEGSs operation. A proper confidence level should be set to realize a balanced tradeoff between system economy, renewable generation accommodation and reliability in practical applications.

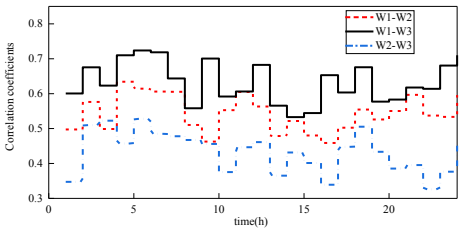

Fig. 3 Hourly correlation coefficients of wind farms

TABLE I

OPERATIONAL COSTS AND SCHEDULED WIND POWER OUTPUT COMPARISON OF DIFFERENT CASES

Period	Case I		Case II	
	Costs/$	Wind power/MW	Costs/$	Wind power/MW
normal wind speed period	1978767	4700	1992279	4281
high wind speed period	1890823	7817	1902124	7384
low wind speed period	2003795	3889	2028744	3483

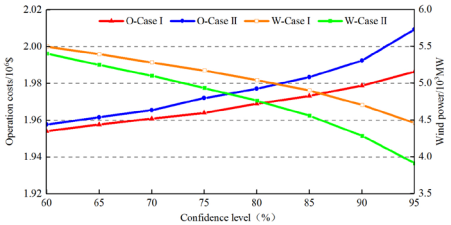

Fig.4 The operational costs and total wind power output under different confidence levels for β_1

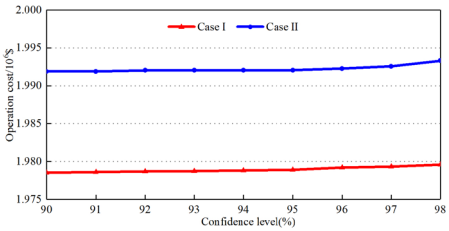

Fig. 5 The operational costs under different confidence levels for β_2, β_3, β_4 and β_5

B. Coordinated Optimization between Dispatch Plan Formulation and Contract Decomposition

In this section, the coordinated optimization between dispatch plan formulation and contract decomposition is analyzed with the consideration of wind power correlation under normal wind speed periods. The confidence level of power balance β_1 is set to 90%, and the reserve and power flow confidence levels β_2, β_3, β_4 and β_5 are all set to 96%.The electricity contract parameters of the bidding units can be found in [23]. Some test cases are designed as follows:

Case III: No consideration of electricity contract decomposition when formulating the day-ahead dispatch plan.

Case IV: The decomposition problem of the electricity contract is introduced into the progress of the dispatch plan formulation, but the case that the daily decomposed electric quantity of the contract may not be executable in the actual dispatch plan are ignored.

Case V: Coordinated optimization between dispatch plan formulation and contract decomposition is considered.

Table II shows the system operational costs and variance of the units' contract completion progress in various cases. Compared to Case III, the operational costs increase from $1,992,279 to $2,110,107 and the variance of the contract completion progress decreases from 6.8529 to 1.7059 in case V. This is due to the relative high generation costs of some bidding units. When the demand of the contract completion progress is involved, the operational costs will increase accordingly. The feasibility of the decomposed electric quantity is not considered in Case IV, and the decomposed electric quantity is not executable in the dispatch plan. Hence, the operational costs are not obtained in Case IV.

The variance of the contract completion progress in Case IV and Case V are 1.5331 and 1.7059, respectively, which are evidently lower than the 6.8529 in Case III. It is revealed that considering the electricity contract decomposition problems when formulating the dispatch plan can reduce the contract completion deviation of different units, so as to improve the fairness of the contract completion schedule plan formulation.

Although the variance of the contract completion progress in case IV is lower than that in Case V, the daily decomposed electric quantity cannot be fully executable in the dispatch plan.

The proposed method in Case V first locates the unit number that shows the decomposed electric quantity is not executable and the non-executable electric quantity in the first decomposition results. As shown in Fig.6, the blue line represents the unit number and corresponding non-executable electric quantities in the first contract decomposition results. G16, G21, G22, G24, G43 and G45 are the units for which the decomposed electric quantity is not executable. Among them, the worst case is the contract decomposition results of unit G43 whose non-executable electric quantity is up to 442 MWh. Through iterative coordinated optimization of the optimal dispatch model and contract decomposition model, the non-executable electric quantity is eliminated, which is shown as a red and black line in Fig.6. It can be observed that the non-executable electric quantity is eliminated through two iterations. The final contract decomposition results are shown in the red bar graph in Fig. 7. As seen, the generation of units which first had decomposed contract energy are non-executable, are reduced, and the reduced power generation are completed by units G27, and G28, which ensures the total power generation of the bidding units on the plan day.

The above analysis shows that considering coordinated optimization between dispatch plan formulation and contract decomposition can provide relatively practical decomposition results, so as to improve the fairness of the contract completion schedule plan formulation and the feasibility of the delivery of the electricity transaction plan into the dispatch plan.

TABLE II
COMPARISON OF OPERATION COSTS AND VARIANCE OF CONTRACT COMPLETION PROGRESS IN DIFFERENT CASE

	Operation costs/$	Variance of contract completion progress
Case III	1992279	6.8529
Case IV	×	1.5331
Case V	2110107	1.7059

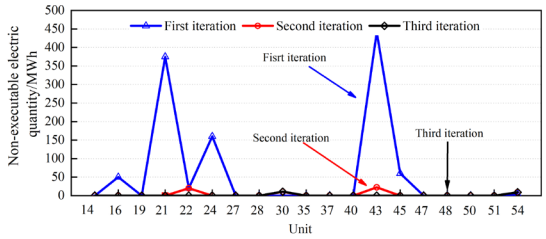

Fig. 6 Non-executable electric quantity varies over number of iterations

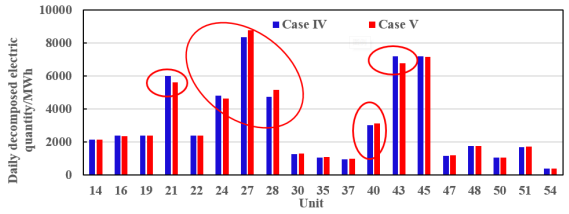

Fig. 7 Results of daily contract decomposition in Case IV and Case V

VI. Conclusion

This paper proposes a novel stochastic optimal dispatch of an IEGS considering wind power correlation and electricity transactions. The influence of wind power uncertainties is modeled as probabilistic chance constraints by using chance-constrained programing. This design can drive the IEGS operation to realize a balanced trade-off between operational costs, wind power utilization and system reliability through setting a reasonable confidence level. Moreover, a coordinated optimization strategy between electricity contract decomposition and day-ahead dispatch plan formulation is developed to provide relatively practical decomposition results, so as to improve the feasibility of the delivery of the electricity transaction plans into the dispatch plan.

Appendix

The gas flow equation (15) can be eased by the second-order cone programming (SOCP) method in [25], the detailed relaxation progress is shown as follows:

$$\prod_i = \pi_i^2,\ \prod_j = \pi_j^2 \tag{44}$$

$$(F_{ij} / C_{ij})^2 = (f_{ij}^+ - f_{ij}^-)(\prod_i - \prod_j) \tag{45}$$

$$-f_{ij}^- \cdot F_{ij}^{\max} \le F_{ij} \le f_{ij}^+ \cdot F_{ij}^{\max} \tag{46}$$

$$f_{ij}^- + f_{ij}^+ \le 1 \tag{47}$$

where f_{ij}^+ and f_{ij}^- are 0-1 variables that represent the gas flow direction of pipeline ij. F_{ij}^{max} represents the maximum allowable gas flow through pipeline ij.

The equation (45) can be further substituted by (48)-(52):

$$(F_{ij} / C_{ij})^2 = \lambda_{ij},\ \ \forall (i,j) \in N_{\text{gas}} \tag{48}$$

$$\lambda_{ij} \ge \prod_j - \prod_i + (f_{ij}^+ - f_{ij}^- + 1)(\prod_i^{\min} - \prod_j^{\max}) \tag{49}$$

$$\lambda_{ij} \ge \prod_i - \prod_j + (f_{ij}^+ - f_{ij}^- - 1)(\prod_i^{\max} - \prod_j^{\min}) \tag{50}$$

$$\lambda_{ij} \le \prod_j - \prod_i + (f_{ij}^+ - f_{ij}^- + 1)(\prod_i^{\max} - \prod_j^{\min}) \tag{51}$$

$$\lambda_{ij} \le \prod_i - \prod_j + (f_{ij}^+ - f_{ij}^- - 1)(\prod_i^{\min} - \prod_j^{\max}) \tag{52}$$

Furthermore, equation (48) can be eased into a standard second-order cone (SOC) relaxation formulation as presented in (53):

$$\left\| \begin{matrix} 2F_{ij} / C_{ij} \\ \lambda_{ij} + 1 \end{matrix} \right\|_2 \le \lambda_{ij} + 1 \tag{53}$$

The final gas flow equation relaxation forms can be represented by (46)-(47) and (49)-(53). However, the accuracy of the relaxation cannot be always guaranteed due to the influence of objective functions and network constraints. Thus, a small penalty item represented by $\delta\lambda_{ij}$ is added to (1) to tighten SOC constraints, in which δ is 0.01.

References

[1] Y. S. Guo, H. H. Kuang, S. Q. Guo, and C. R. Yang, "Research on weekly unit commitment strategy harmonizing long term market trade planning and daily generation scheduling," *Power System Protection and Control*, vol. 45, no. 22, pp. 78–82, Nov. 2017.

[2] S. M. Miao, B. Luo, J. J. Shen, C. T. Cheng, G. Li, and Y. J. Sun, "Short-term multi-objective hydro-thermal generation dispatch considering electricity market transition and mid-and long-term contract decomposition," *Power System Technology*, vol. 42, no. 7, pp. 2221–2231, Jul. 2018.

[3] L. L. Li, Y. B. Guan, J. Geng, J. G. Yao, and G. Wang, "Modeling and solving for monthly security constrained unit commitment problem," *Automation of Electric Power Systems*, vol. 35, no. 12, pp. 27 - 31, 64, Jun. 2011.

[4] X. R. Wu, Y. Li, Y. Tan, Y. J. Cao, and C. Rehtanz, "Optimal energy management for the residential MES," *IET Generation, Transmission & Distribution*, vol. 13, no. 10, pp. 1786–1793, May 2019, doi: 10.1049/iet-gtd.2018.6472.

[5] A. Alabdulwahab, A. Abusorrah, X. P. Zhang, and M. Shahidehpour, "Coordination of interdependent natural gas and electricity infrastructures for firming the variability of wind energy in stochastic day-ahead scheduling," *IEEE Transactions on Sustainable Energy*, vol. 6, no. 2, pp. 606–615, Apr. 2015.

[6] R. F. Zhang, T. Jiang, G. Q. Li, H. H. Chen, X. Li, L. Q. Bai, and H. T. Cui, "Day-ahead scheduling of multi-carrier energy systems with multi-type energy storages and wind power," *CSEE Journal of Power and Energy Systems*, vol. 4, no. 3, pp. 283–292, Sep. 2018.

[7] Y. Li, L. He, F. Liu, C. B. Li, Y. J. Cao, and M. Shahidehpour, "Flexible voltage control strategy considering distributed energy storages for dc distribution network," *IEEE Transactions on Smart Grid*, vol. 10, no. 1, pp. 163–172, Jan. 2019.

[8] E. A. Martínez Ceseña and P. Mancarella, "Energy systems integration in smart districts: Robust optimisation of multi-energy flows in integrated electricity, heat and gas networks," *IEEE Transactions on Smart Grid*, vol. 10, no. 1, pp. 1122–1131, Jan. 2019.

[9] D. Huo, C. H. Gu, K. Ma, W. Wei, Y. Xiang, and S. Le Blond, "Chance-constrained optimization for multienergy hub systems in a Smart city," *IEEE Transactions on Industrial Electronics*, vol. 66, no. 2, pp. 1402–1412, Feb. 2019.

[10] Y. Shui, H. J. Gao, L. F. Wang, Z. B. Wei, and J. Y. Liu, "A data-driven distributionally robust coordinated dispatch model for integrated power and heating systems considering wind power uncertainties," *International Journal of Electrical Power & Energy Systems*, vol. 104, pp. 255–258, Jan. 2019.

[11] Y. Xiang, J. Y. Liu, and Y. L. Liu, "Robust energy management of microgrid with uncertain renewable generation and load," *IEEE Transactions on Smart Grid*, vol. 7, no. 2, pp. 1034–1043, Mar. 2016.

[12] Q. F. Wang, Y. P. Guan, and J. H. Wang, "A chance-constrained two-stage stochastic program for unit commitment with uncertain wind power output," *IEEE Transactions on Power Systems*, vol. 27, no. 1, pp. 206–215, Feb. 2012.

[13] P. Velarde, L. Valverde, J. M. Maestre, C. Ocampo-Martinez, and C. Bordons, "On the comparison of stochastic model predictive control strategies applied to a hydrogen-based microgrid," *Journal of Power Sources*, vol. 343, pp. 161–173, Mar. 2017.

[14] Y. Li, Z. Yang, G. Q. Li, D. B. Zhao, and W. Tian, "Optimal scheduling of an isolated microgrid with battery storage considering load and renewable generation uncertainties," *IEEE Transactions on Industrial Electronics*, vol. 66, no. 2, pp. 1565–1575, Feb. 2019.
[15] Z. Wu, P. L. Zeng, X. P. Zhang, and Q. Y. Zhou, "A solution to the chance-constrained two-stage stochastic program for unit commitment with wind energy integration," *IEEE Transactions on Power Systems*, vol. 31, no. 6, pp. 4185–4196, Nov. 2016.
[16] M. Lubin, Y. Dvorkin, and S. Backhaus, "A robust approach to chance constrained optimal power flow with renewable generation," IEEE Transactions on Power Systems, vol. 31, no. 5, pp. 3840–3849, Sep. 2016.
[17] J. Z. Liu, H. Chen, W. Zhang, B. Yurkovich, and G. Rizzoni, "Energy management problems under uncertainties for grid-connected microgrids: A chance constrained programming approach," IEEE Transactions on Smart Grid, vol. 8, no. 6, pp. 2585–2596, Nov. 2017.
[18] L. Feng, J. N. Zhang, G. J. Li, and B. L. Zhang, "Cost reduction of a hybrid energy storage system considering correlation between wind and PV power," *Protection and Control of Modern Power Systems*, vol. 1, no. 1, pp. 11, Dec. 2016.
[19] Z. Wang, W. S. Wang, C. Liu, Z. Wang, and Y. H. Hou, "Probabilistic forecast for multiple wind farms based on regular vine copulas," *IEEE Transactions on Power Systems*, vol. 33, no. 1, pp. 578–589, Jan. 2018.
[20] D. F. Cai, D. Y. Shi, and J. F. Chen, "Probabilistic load flow computation using Copula and Latin hypercube sampling," *IET Generation, Transmission & Distribution*, vol. 8, no. 9, pp. 1539–1549, Sep. 2014.
[21] M. F. Ban, J. L. Yu, M. Shahidehpour, and Y. Y. Yao, "Integration of power-to-hydrogen in day-ahead security-constrained unit commitment with high wind penetration," *Journal of Modern Power Systems and Clean Energy*, vol. 5, no. 3, pp. 337 – 349, May 2017.
[22] M. Madrigal and A. D. Quintana, "Semidefinite programming relaxations for {0,1}-power dispatch problems," in *Proceedings of 1999 IEEE Power Engineering Society Summer Meeting*, Edmonton, Canada, Jul. 697 – 702, 1999.
[23] G. Wu. (2019. Apr.). Case Study Parameter. [Online]. Available: https://github.com/scugw/Case-Study-Parameter/blob/master/IEGS_ET_Data.pdf
[24] National Oceanic and Atmospheric Administration. NBDC Standard Meteorological Buoy Data. [Online]. Available: https://coastwatch.pfeg.noaa.gov/erddap/tabledap/index.html?page=1&itemsPerPage=1000.
[25] S. Chen, Z. N. Wei, G. Q. Sun, D. Wang, and H. X. Zang, "Steady state and transient simulation for electricity-gas integrated energy systems by using convex optimisation," *IET Generation, Transmission & Distribution*, vol. 12, no. 9, pp. 2199–2206, May 2018

Gang WU is a M.S. candidate at the College of Electrical Engineering, Sichuan University, China. His research interests include optimal operations of integrated energy systems.

Yue Xiang (S'12-M'16) received his B.S. and Ph.D. degrees from Sichuan University, China, in 2010 and 2016, respectively. Currently he is an associate professor at the College of Electrical Engineering, Sichuan University, China. His main research interests are power system planning and optimal operations, renewable energy integration.

Junyong Liu (M'17) received his Ph.D. degree from Brunel University, UK, in 1998. He is a professor at the College of Electrical Engineering, Sichuan University, China. His main research areas of interest are the power market, power system planning and operations.

Xin Zhang (M'17) received his B.Eng. degree in automation from Shandong University, China, in 2006; his M.Sc. and Ph.D. degrees in electrical power engineering from The University of Manchester, U.K., in 2007 and 2010 respectively. He is a Senior Lecturer (Associate Professor) in energy systems at Cranfield University, U.K. His recent research activities include sustainable energy systems for the electrification of airports and aviation. From 2011 to 2019, he was a Power System Engineer at the National Grid U.K., where he held various roles including national energy strategy, power system analysis and power market operations, primarily in the GB Electricity National Control Centre. His research interests include power system planning and operations.

Shuoya TANG is a PhD candidate at the College of Electrical Engineering, Sichuan University, China. Her main research areas of interest are distribution system planning, electric vehicle prediction, interaction between electric vehicles and distribution systems.